Excited State Equilibration in the Photosystem I−Light-Harvesting I Complex: P700 Is Almost Isoenergetic with Its Antenna

Roberta Croce,[‡] Giuseppe Zucchelli,[‡] Flavio M. Garlaschi,[‡] Roberto Bassi,[§] and Robert C. Jennings*[,‡]

Centro CNR Biologia Cellulare e Molecolare delle Piante, Dipartimento di Biologia, Università di Milano, via Celoria 26, 20133 Milano, Italy, and Laboratorio di Fotosintesi, Facoltà di Scienze MM. FF. NN., Università di Verona, Strada Le Grazie- Cà Vignal, 37134 Verona, Italy

Received January 29, 1996; Revised Manuscript Received April 8, 1996[⊗]

ABSTRACT: Photosystem I with its full antenna complement (PSI−LHCI) has been prepared by mild detergent solubilization with octyl β-D-glucopyranoside from maize thylakoids. A preliminary polypeptide analysis is presented. At room temperature, the steady-state fluorescence derives from an almost perfectly thermalized state, as demonstrated by a Stepanov analysis, in which about 90% of the excited states are associated with the red chlorophyll spectral forms absorbing above 700 nm. Equilibration is temperature-sensitive and is lost at $T < 200$ K. A careful analysis of fluorescence between 75 and 280 K clearly demonstrates the presence of at least three red chlorophyll spectral forms with emission maxima at 720, 730, and 742 nm, the absorption origin bands of which have been calculated at 714, 725, and 738 nm. On the basis of a minor deviation from thermal equilibration around 695 nm, it is suggested that at least 3−4 antenna chlorophylls, with an average absorption near 695 nm, are strongly coupled to P700. Thermodynamic analysis of absorption and fluorescence spectra indicates that the equilibrium, absorption-weighted excited state population of the P700 dimer is around 0.013 assuming that the low-energy exciton state possesses all the oscillator strength. The average free energy for excitation transfer from antenna to P700 is thus calculated to be −0.26 kT at room temperature. This indicates that P700 is almost isoenergetic with its antenna at room temperature when the red forms are taken fully into account. From the calculated excited state population of P700, we estimate that the primary charge separation rate in PSI is 1−2 ps^{-1}.

Photosystem I is a supramolecular complex located in the nonappressed thylakoid membranes. The complex binds P700 and can photoreduce ferredoxins and oxidize plastocyanin (Bruce & Malkin, 1988). The complex is composed of two moieties: (1) a chlorophyll (chl)[1] *a* binding core complex and (2) a chl *a/b* binding peripheral antenna called LHCI. The products of the *PsaA* and *PsaB* chloroplast genes are the major 60 kDa subunits of the core complex and bind all of the approximately 90 chl *a* and 14 β-carotene molecules (Sieferman-Harms & Ninneman, 1982; Bassi & Simpson, 1987) besides P700 as well as the primary acceptors A0 and A1 at the interface between the 2 homologous subunits (Goldbeck, 1992). Several small polypeptides (up to 10) have been detected as components of the PSI core acting in binding of iron sulfur centres (PsaC) or involved in interactions with other thylakoid complexes [for a review, see Chitnis et al. (1995)].

The LHCI moiety is arranged around the core (Boekema et al., 1990) and is composed of the products of four, nuclear genes, *Lhca* 1−4, with MW of 20−24 kDa. It binds about 110 chl *a*+*b* and approximately 20 xanthophyll molecules (Lam et al., 1984; Bassi & Simpson, 1987). The PSI−LHCI complex can be isolated in an intact form which has a chl/P700 ratio of about 210 when the complex is extracted from higher plants and absorbs maximally at 680 nm (Mullet et al., 1980; Bassi & Simpson, 1987). Its absorption spectrum is characterized by a significant absorption in the long-wavelength tail, suggesting the presence of the red spectral chlorophyll forms absorbing at lower energies than the primary donor P700. It is usually reported that these pigments largely determine the steady-state emission properties at low temperatures, whereas at RT their emission is generally considered to be weak and difficult to distinguish from that of the bulk antenna chls (e.g., Werst et al., 1992). Two pigments pools with red-shifted emissions near 720 and 735 nm are generally reported for higher plant PSI at cryogenic temperatures (Mullet et al., 1980; Wittmershaus, 1986; Mukerji & Sauer, 1989; Pålsson et al., 1995) though even longer wavelength emission has been described in cyanobacteria (Shubin et al., 1995). Over the past decade, many attempts have been made to determine the origin absorption bands of these red-shifted emission forms. In most reports, the 720 nm fluorescence is proposed to be associated with a 695 nm absorption band and the 735 nm emission with an approximately 705 nm absorption (e.g., Wittmershaus, 1986). The 760 nm emission in *Spirulina platensis* has been suggested to originate from a 735 nm absorption band (Shubin et al., 1995). Thus, it is clear that the suggested values for the Stokes shifts (15−25 nm approximately) for the red forms are rather large. For chls in organic solvents, values of around 4−8 nm are usually reported (Zscheile & Harris, 1947; Seely & Connolly, 1986) whereas for chl *a* spectral forms in chl−protein complexes, Stokes shifts of 1−4 nm are suggested (Hayes et al., 1988;

* Address correspondence to this author.
‡ Università di Milano.
§ Università di Verona.
⊗ Abstract published in *Advance ACS Abstracts,* May 15, 1996.
[1] Abbreviations: chl, chlorophyll; FWHM, full width at half-maximum. LHC, light-harvesting complex; MW, molecular mass; OGP, octyl β-D-glucopyranoside; PSI, photosystem I; PSII, photosystem II; RC, reaction center; RT, room temperature; *k*, Boltzmann constant.

S0006-2960(96)00214-0 CCC: $12.00

Zucchelli et al., 1992). These very large proposed values for the Stokes shifts may therefore indicate that the red forms possess rather unusual spectroscopic properties possibly associated with very strong electron−phonon coupling, as has been previously suggested (Gobets et al., 1994).

Time-resolved spectroscopic studies indicate that the overall trapping time in PSI is in the 50−120 ps range (Holzwarth, 1986; Hodges & Moya, 1986; Owens et al., 1987; Turconi et al., 1994), with faster times (*circa* 30 ps) for core particles (Holzwarth et al., 1993). The transfer time from the bulk antenna to red forms has been determined to be in the 4−12 ps range (Turconi et al., 1994), and trapping occurs from a state in which fluorescence from the red forms dominates. This state is generally considered to be a thermally equilibrated state, and this forms the basis for several attempts at determining the intrinsic charge separation rate constant (Trissl, 1993; Hastings et al., 1994). We would, however, point out that a rigorous demonstration of thermal equilibration requires a detailed comparison between absorption and fluorescence spectra (Zucchelli et al., 1995a) and as such experiments have not yet been published for PSI this aspect remains to date unresolved. It should however be mentioned that Ross and Calvin (1967) did in fact attempt such an analysis for PSI using chloroplast action spectra. However, it is well-known that action spectra are usually substantially distorted with respect to absorption spectra and at best can yield an absorbance (not extinction) band shape.

As mentioned above, the absorption maximum of the PSI antenna is near 680 nm, whereas the primary donor P700 is energetically lower by about twice the thermal energy (kT) at room temperature. On the other hand, for PSII the primary donor (P680) is only very slightly lower than the antenna absorption (*circa* 0.5 kT). This interesting property of PSI−RC is expected to lead to a rather high probability of an exciton residing on P700 which has been approximated, on the basis of thermodynamic equilibrium considerations, to be between 0.06 and 0.1 (Jennings et al., 1996, Trissl, 1993). On the other hand, for P680 this value is much lower and in the range 0.01−0.02 (Jennings et al., 1994a). It has been suggested that this is the main reason for fast photochemical trapping in PSI (Trissl, 1993; Jennings et al., 1996). These conclusions, however, are based on the assumption of thermal equilibration over the entire antenna−RC matrix, which as pointed out above has not been experimentally demonstrated to date. In most published PSI emission spectra at RT, the dominant band is around 680−690 nm, seemingly associated with the bulk antenna absorption. This is not in agreement with what would be expected from an equilibrium distribution of excited states when the red absorption forms are taken into consideration. It is easily demonstrated, as shown by Trinkunas and Holzwarth (1994) for a PSI core complex, that the dominant fluorescence band should be associated with the red forms. The reason for the apparently blue-shifted emission of most PSI samples could be due to either (1) a nonequilibrium distribution of excited states or (2) the presence of energetically uncoupled chlorophylls with high fluorescence yield and a relatively "blue" emission (near 680 nm). In the present study, we analyze this aspect in detail. It is demonstrated that under appropriate incubation conditions and using a novel PSI−LHCI particle prepared by very mild OGP solubilization of thylakoid membranes, the steady-state emission is almost perfectly thermally equilibrated in the 200−300 K temperature range, with RC trapping provoking a limited spectral perturbation near 695 nm. Under these conditions, about 90% of the excited states are localized in the red forms, of which three are clearly identified. Our analysis furthermore demonstrates that, contrary to the general expectation, P700 is not a "deep trap" but is almost isoenergetic with its antenna when all the red forms are taken into consideration.

MATERIALS AND METHODS

Purification of PSI−LHCI. Leaves of 15-day-old *Zea mays* were homogenized in 0.4 M sorbitol, 0.1 M Tricine, pH 7.8, 10 mM NaCl, and 5 mM $MgCl_2$. Isolation of the thylakoids was performed as described previously (Bassi & Simpson, 1987). Freshly prepared thylakoids were resuspended at 1 mg/mL chl in distilled water and solubilized by octyl β-D-glucopyranoside (OGP) at a final concentration of 2%. After stirring for 30 min at 4 °C, the sample was centrifuged for 10 min at 40000*g*, and 1.5 mL aliquots of supernatant were loaded into ultracentrifuge tubes containing 12 mL of a 10−40% sucrose gradient layered over a 1 mL cushion of 2 M sucrose at the bottom of the tube, also containing 5 mM Tricine, pH 7.8, and 0.8% OGP. After centrifugation for 21 h at 41 000 rpm in an SW41 rotor (Beckman) at 4 °C, six chlorophyll-containing bands are distinguished. The bands were collected and analyzed on SDS−PAGE. The lowermost band, containing PSI−LHCI, was dialyzed overnight against 5 mM Tricine, pH 7.8 at 4 °C, and centrifuged for 2 h at 60 000 rpm in an 80Ti rotor (Beckman). The pellet, PSI particles, was resuspended in 50 mM sorbitol and 5 mM Tricine, pH 7.8, and frozen in liquid nitrogen prior to storing at −80 °C.

Stroma lamellae were prepared by Yeda press fractionation according to Bassi et al. (1988).

The chlorophyll *a/b* ratios of the PSI−LHCI and stroma lamellae preparation were, respectively, 12 and 7.8 as determined by the method of Porra et al. (1989).

One- and Two-Dimensional Electrophoresis. SDS−6 M urea−PAGE was performed in Tris−sulfate buffer as previously reported (Bassi et al., 1987) in a 12−18% acrylamide gradient on a 160 × 120 × 1.5 mm gel slab. For two-dimensional analysis, a gel line from Tris−sulfate−PAGE was excised and re-run on a 12−18% acrylamide gradient gel with the buffer system described by Schägger and von Jagow (1987).

Absorption and Fluorescence Spectroscopy. The absorption and fluorescence emission spectra were measured at 6 °C using an EG & G OMAIII (Model 1460) with an intensified diode array (Model 1420) mounted on a spectrograph (Jobin-Yvon HR320) with a 150 groove mm^{-1} grating. For the absorption measurements, 30 000 spectra were accumulated with other conditions the same as previously reported (Jennings et al., 1993). Fluorescence was excited at 475 nm, FWHM 2 nm, and measured at 90° after being filtered by an OG530 filter (Schott). Each spectrum has about 20 000 counts at the maximum. A 3 × 3 mm cuvette was used. The sample was diluted to an optical density of 0.03 at 681 nm in 5 mM Tricine, pH 7.8. The emission spectra were corrected for instrumental distortion using an intensity-calibrated source (ISCO Spectroradiometer calibrator). For low-temperature measurements, a vacuum-assisted Joule−Thomson refrigerating system (Model K-2002T, MMR Technologies, Inc.) was used. The buffer for the low-temperature measurements contained 60% glycerol.

Fluorescence excitation spectra were recorded using an SLM fluorometer (Model 4800S, Urbana, IL) at several different emission wavelengths. The FWHM values of the emission and excitation monochromators were 8 nm and 2 nm, respectively. Spectra were corrected using a rhodamine quantum counter. Spectra were recorded at 6 °C.

Decomposition analysis of the spectra in terms of "asymmetric" Gaussian bands was performed as previously described (Zucchelli et al., 1990) using a nonlinear least-squares algorithm that minimizes the χ^2 function with respect to the parameters of a model function. This model function is written as a weighted sum of a variable number of "asymmetric" Gaussian curves.

Electron Transport. Methyl viologen reduction was assayed using a PHM 72 Mk2 oxygraph (Radiometer Copenhagen). The 2 mL reaction mixture contained dichlorophenolindophenol (16 μM), sodium ascorbate (2.5 mM), methyl viologen (100 μM), and PSI−LHCI containing 50 μg of chlorophyll in 5 mM Tricine, pH 7.8, buffer. Illumination was with interference filters (Balzers B-40; FWHM 10 nm) with peak transmission values at 740 and 750 nm. The light intensity was measured with a Yellow Springs radiometer. The filter transmission was analyzed in the OMA spectrophotometer.

Fluorescence Yield. The fluorescence yield was determined by integration of the emission area of the instrument-corrected spectra between 650 and 800 nm in the absence and presence of Triton X-100 (5%), with 440 nm excitation. Assuming a monomer chlorophyll emission yield of 33% (Ide et al., 1987; Sopko et al., 1995), we estimated the fluorescence yield for the PSI−LHCI preparation to be about 0.5% in the absence of detergent.

RESULTS

In the present study, we have analyzed a PSI−LHCI preparation obtained by mild detergent extraction with OGP. This detergent, as distinct from others commonly used, may be completely removed from the preparation and thus allows its concentration to be controlled (Baron & Thompson, 1975).

The chl *a/b* ratio was consistently found to be 12 using the method of Porra (1989). This is similar to previously reported preparations of this type (Mullet et al., 1980; Bassi et al., 1985; Bassi & Simpson, 1987; Tjus et al., 1994) when the values obtained by the commonly used Arnon (1949) procedure are converted to those of the Porra method. The polypeptide composition was analyzed by SDS−urea PAGE (Figure 1A), showing that the preparation was completely free of contamination by other thylakoid components such as PSII or LHCII. It is worth noting that the relative amount of PSI−LHCI polypeptides (Figure 1A, lane 4) is very similar to that found in the stroma membrane preparation (lane 3), thus suggesting that there was no detachment of PSI−LHCI components during purification. Figure 1B shows a more detailed analysis of polypeptide composition in the low MW range by two-dimensional SDS−PAGE. In the range between 8 and 24 kDa, at least 17 polypeptides were resolved, and 7 were identified by immunoblotting with specific antibodies (data not shown) as indicated in Figure 1 A,B.

The RT fluorescence emission spectra of PSI−LHCI, measured in the presence of different detergent concentrations, are presented in Figure 2. In the absence of detergent, the main emission band is broad and has its maximum at

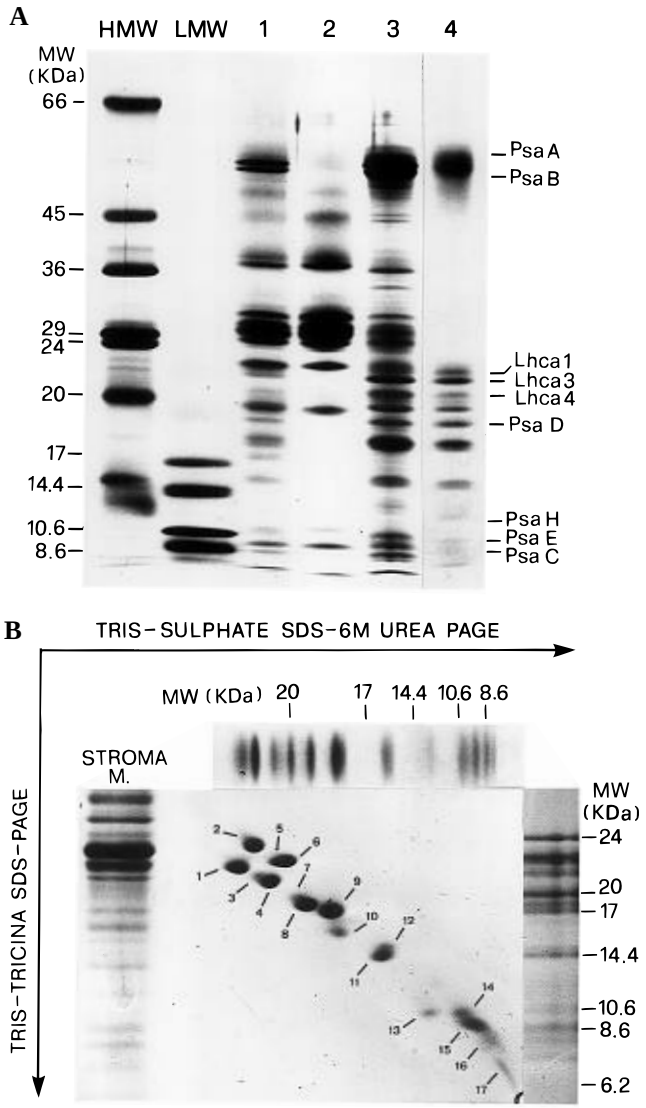

FIGURE 1: One-dimensional (A) and two-dimensional (B) SDS−PAGE analysis of PSI−LHCI. (A) Tris−sulfate SDS−6 M urea−PAGE in 12−18% acrylamide gradient. Lane 1, thylakoids. Lane 2, PSII membranes (BBY). Lane 3, stroma lamellae (SL). Lane 4, PSI−LHCI. (B) Tris−Tricine SDS−PAGE in 12−18% acrylamide gradient. Lane 1, stroma lamellae. Lane 2, two-dimensional fractionation of the low MW region of the PSI complex in panel A. Lane 3, PSI−LHCI. The identified polypeptides are (1) Lhca4, (2) Lhca3, (3) Lhca1, (8) PsaD, (13) PsaH, (14) PsaE, and (15) PsaC.

722 nm. A shoulder is present in the 680−690 nm range. The effect of detergent is clearly to increase markedly the contribution of the emission band near 680 nm. We demonstrate below (Figure 3) that this is due to detergent-induced uncoupling of chl *a* from the PSI complex. We note that most published RT spectra for PSI−LHCI are similar to the spectra e, f, and g.

In order to determine whether contact with detergent induced energetic uncoupling of single chl *a* molecules or of the LHCI−680 complex from PSI−LHCI, we measured fluorescence excitation spectra by exciting in the blue (400−550 nm) and measuring at 680 nm in the presence or absence of detergent (Figure 3). Previously Nechushtai et al. (1986) have studied detergent effects on PSI. The spectra, which have been normalized near the chl *a* absorption maximum at 440 nm, show that detergent leads to a relative decrease in the excitation in the spectral interval dominated by carotenoid and chl *b* absorption (460−520 nm) and a relative increase in the chlorophyll *a* dominated interval (400−450

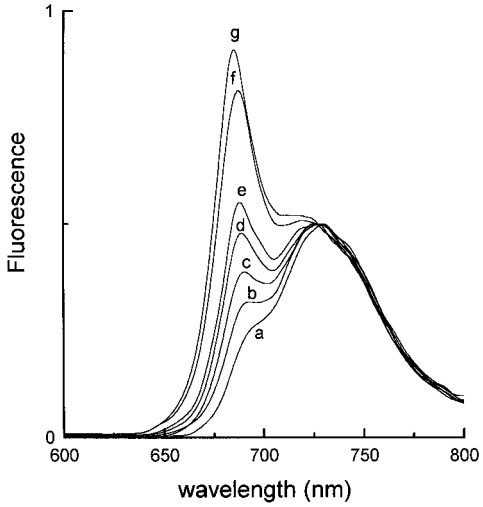

FIGURE 2: Fluorescence spectra of PSI−LHCI at RT in 50 mM sorbitol, 5 mM Tricine, pH 7.8, at different OGP concentrations: 0%, 0.1%, 0.2%, 0.3%, 0.4%, 0.5%, 0.7% (a−g, respectively). The spectra are normalized at 727 nm.

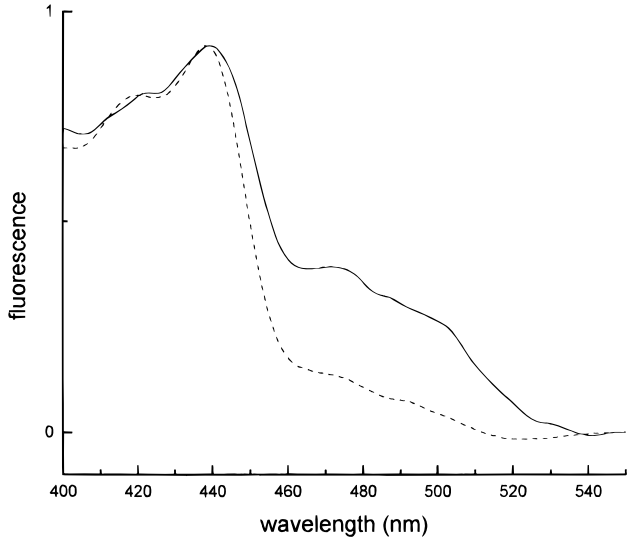

FIGURE 3: Fluorescence excitation spectra of PSI−LHCI between 400 and 550 nm with the emission wavelength at 680 nm. Spectra were measured either in the absence of detergent (solid line) or in the presence of 0.7% OGP (dashed line). The spectra are normalized at 436 nm.

nm). As the 680 nm emission is due to chlorophyll *a*, we interpret these data as detergent bringing about the uncoupling of chl *a* molecules. The greatly increased fluorescence at 680 nm due to detergent treatment (Figure 2) is due to the expected high fluorescence yield of such uncoupled chls. Any LHCI uncoupling is expected to be slight as little structure is present in the 460−520 nm region in detergent-treated samples. This is clear evidence that the emission spectrum in the presence of detergent is not a "native" PSI fluorescence spectrum.

In Figure 4, the problem of thermal equilibration is addressed by comparing the measured emission spectrum with that calculated from the absorption spectrum utilizing the Stepanov relation $[(F(\nu)/A(\nu) = C(T)\nu^3 \exp[-(h\nu/kT)]]$ for different temperatures. This expression connects absorption and fluorescence spectra in a system in which thermal equilibration between all energy levels is attained. For the reasons discussed above, this analysis has been performed on samples resuspended in the absence of detergent and in which P700 is presumably oxidized due to the continuous

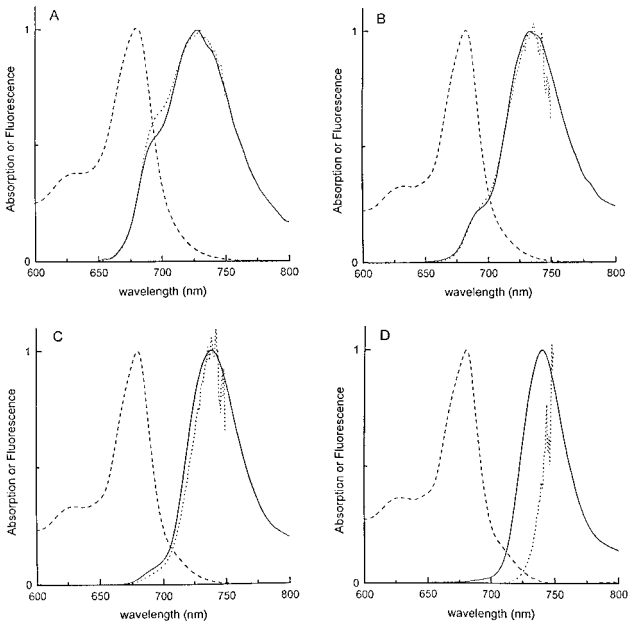

FIGURE 4: Comparison between calculated (dotted line) and measured (solid line) fluorescence spectra for PSI−LHCI at 280 K (A), 225 K (B), 175 K (C), and 100 K (D). Emission spectra were calculated from the measured absorption spectra (dashed line) by the Stepanov equation.

illumination. The analysis at RT (Figure 4A) shows that rather good agreement is encountered between the measured and calculated emission spectra over most of the interval 640−750 nm, though a deviation near 695 nm is apparent which is discussed below. In both cases, the RT emission maximum is near 720 nm with a shoulder in the 680−690 nm region. This shoulder is associated with the bulk antenna which absorbs maximally at 681 nm. The broad red emission peaking near 720 nm, which accounts for about 90% of the integrated fluorescence intensity at RT, is due to the minor red spectral forms clearly evident in the absorption spectrum.

Figure 4B−D shows the absorption/fluorescence analysis for 225, 175, and 100 K. While the expected "thermodynamic" red shifting of the emission spectrum upon lowering the temperature is evident, the Stepanov calculations show that below about 200 K thermal equilibration is not attained on a sufficiently fast time scale with respect to trapping to show up in steady-state measurements.

A complete set of emission spectra for the temperature range 75−280 K is presented in Figure 5. Of particular interest in this figure is the presence of at least three emission structures in the main red band at approximately 720, 730, and 740 nm. Similar observations have been made on detergent-incubated samples (data not shown). While the two shorter wavelength structures seem similar to the approximately 720 and 735 nm emissions noticed previously (Mullet et al., 1980; Wittmershaus, 1986; Mukerji & Sauer, 1989; Pålsson at al., 1995), the demonstration of a clear emission structure in higher plant PSI near 740 nm seems to be novel. We would point out that while this structure is most evident at 75 K, where it represents the emission maximum, it is also present at RT as a long-wavelength shoulder. The thermodynamic analysis of Figure 4A shows that even this red-most emission is from a thermally equilibrated state at RT.

In an attempt to more precisely define these three emission structures, we subjected the emission spectra presented in Figure 5 to a Gaussian decomposition analysis. A Gaussian

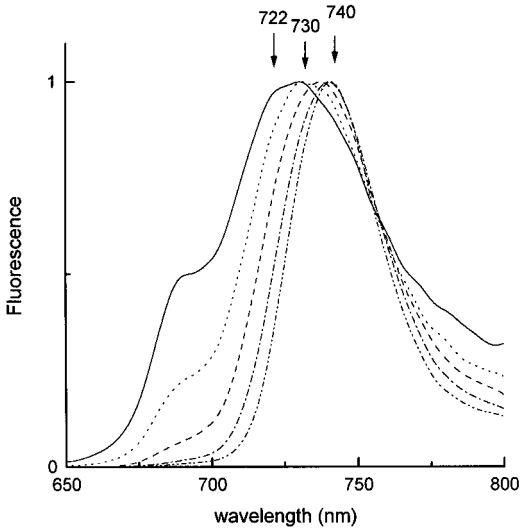

FIGURE 5: Fluorescence spectra of PSI−LHCI in 5 mM Tricine, pH 7.8, and 60% glycerol measured at different temperatures: 270 K (solid line), 225 K (dotted line), 175 K (dashed line), 125 K (dotted−dashed line), and 75 K (dashed−dotted−dotted line). Numbered arrows indicate the approximate wavelength positions of the fluorescence structures.

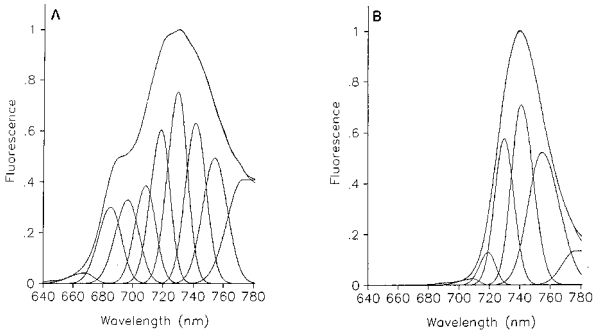

FIGURE 6: Gaussian subband decomposition of fluorescence spectra measured at 270 K (A) and 75 K (B). The sum of Gaussians is also shown.

description was sought which was stable in the sense that the band positions should remain approximately constant in this temperature range. In Figure 6, results of such an analysis are presented for two extreme temperatures. While the Gaussian model to describe fluorescence bands is clearly an oversimplification due to the presence of quite strong vibrational bands from the shorter wavelength emission forms overlapping with the longer wavelength 0−0 transitions, we feel this analysis to be meaningful as at low temperatures the short-wavelength bands are largely suppressed (Figure 6B). Thus, we conclude that the red band emission structures are associated mainly with fluorescence bands with maxima at 720, 730, and 742 nm. We do not wish to attribute any particular physical meaning to the shorter wavelength bands at 270 K as they fall in a largely structureless region of the spectrum. They do, however, provide a good numerical description. This analysis also suggests the presence of emission band(s) at even longer wavelengths. We prefer, however, not to further comment on this possibility for the time being as analysis is complicated by the above-mentioned problem of vibrational bands as well as our inability to detect significant absorption in this wavelength region. It is interesting to note that the three long-wavelength Gaussians have half-bandwidths in the 15−17 nm range and seem to be almost temperature-insensitive, thus suggesting substantial site inhomogeneous broadening (see Discussion). In an

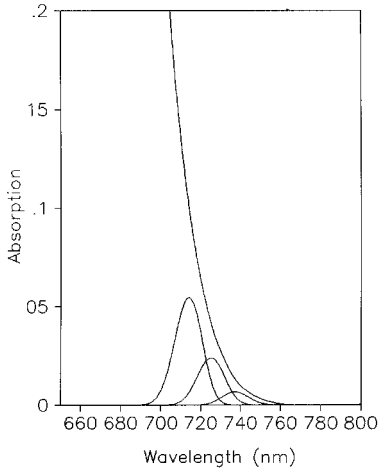

FIGURE 7: Absorption bands calculated from the three red emission bands (720, 730, and 742 nm) using the Stepanov equation. The tail of the absorption spectrum at RT is also shown.

attempt to define the origin bands of these three long-wavelength emissions, we have made use of the fact that emission over this spectral region is thermally equilibrated. Thus, one may use the Stepanov expression to calculate the absorption bands. This has been done for the RT situation, and the results are presented under the long-wavelength absorption tail in Figure 7. The data presented clearly refer only to the homogeneously and inhomogeneously broadened Q_y zero−zero transition. No attempt is made to represent vibrational structure. Thus, we suggest that the 720, 730, and 742 nm emission bands originate from 714, 725, and 738 nm absorption bands, respectively. The Stokes shifts for these inhomogeneously broadened bands are thus between 4 and 6 nm. On a 200 chls per PSI basis, we estimate an approximate area-based stoichiometry of 6, 3, and 1 molecules in ascending wavelength order.

The above results suggest the presence of a number of very substantially red-shifted chl absorption forms in which excitation is thermally equilibrated at RT. This conclusion is at first sight rather surprising as the red-most forms are energetically lower than P700 by between 2−4 kT and 4−6 kT lower than the bulk antenna. As described under Materials and Methods, the fluorescence yield of this preparation is 0.5%, which suggests an overall fluorescence lifetime of less than 100 ps. Thus, it is expected that the quantum efficiency of primary photochemistry for energy absorbed by these red forms should be high. To investigate this, we have determined the quantum efficiency of methyl viologen reduction by exciting in the red absorption tail with 740 and 750 nm interference filters (see Materials and Methods). The sample absorption for PSI-LHCI with these filters is shown in Figure 8. Our measurements yielded values for the per electron quantum efficiency which varied in the range 70−100%, thus bearing out our prediction.

We now address the problem, briefly mentioned above, with reference to Figure 4, that a deviation from thermal equilibration at RT occurs in the wavelength range 680−710 nm. In Figure 9, the same fluorescence data as in Figure 4 are represented together with the ratio of measured to calculated spectra. It is clear from the Stepanov equation that this ratio is proportional to the fluorescence yield [$F(\lambda)$/$A(\lambda)$] at each wavelength. The data in Figure 9 thus show that the fluorescence yield is minimal around 695 nm. The exact position of this minimum varies between 693 and 696 nm for different PSI−LHCI preparations. As the fluores-

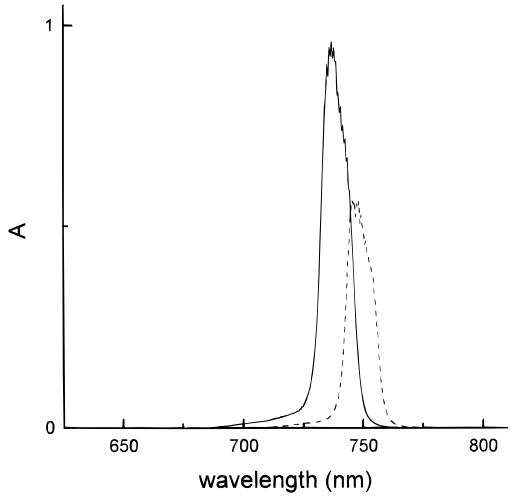

FIGURE 8: Light absorption by PSI−LHCI with two different interference filters at 740 and 750 nm. The spectra (A_λ) were calculated by multiplying the sample absorbance $(1 - T)_\lambda$ by the transmittance spectrum (F_λ) of each filter [$A_\lambda = (1 - T)_\lambda F_\lambda$].

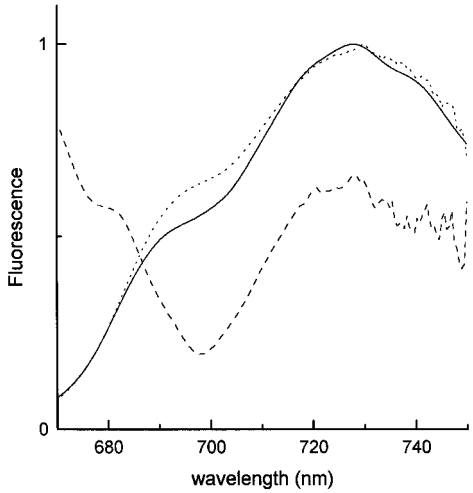

FIGURE 9: Comparison between the measured (solid line) and Stepanov-calculated (dotted line) emission spectra at 280 K. The dashed line represents the ratio of the measured to calculated spectra (×3).

cence yield in PSI is largely determined by RC trapping, we suggest that this behavior is associated with a perturbation of thermal equilibration generated by P700 trapping in chls closely associated with, and including, P700.

DISCUSSION

In the present study, we have undertaken a thermodynamic analysis of the absorption and fluorescence spectra of a PSI−LHCI sample prepared by mild (OGP) solubilization. The choice of this detergent was dictated by the possibility of its being completely removed (Baron & Thompson, 1975) from the sample, a characteristic which is not shared by other such commonly used detergents as dodecyl maltoside and Triton X-100. It is demonstrated that, with the exception of a deviation around 695 nm, the steady-state fluorescence is from a thermally equilibrated state for $T > 200$ K only when detergent is absent from the sample. Under these conditions, over 90% of the emission intensity at RT is associated with the minor red spectral forms absorbing between 705 and 750 nm. The presence of these same minor red forms was demonstrated also for PSI stroma lamellae (unpublished data), thus excluding the possibility that they are produced by the experimental conditions used here. This result is not in agreement with most other published steady-state emission spectra in which the dominant emission band at RT is associated with the bulk chl, which has an average absorption maximum near 680 nm. We interpret this discrepancy to the extreme sensitivity of PSI−LHCI to detergent, which we show here leads to a large increase in fluorescence from uncoupled chls. Apparently, insufficient attention has been paid to this aspect in the past. The very close agreement which we demonstrate, between the measured fluorescence spectrum and that calculated with the Stepanov expression, strongly supports our conclusion that at RT most fluorescence is from the minor red forms. This extreme red-shifted, but thermally equilibrated, emission may be a property of the intact PSI−LHCI particle as it does not seem to be present in PSI core membranes prepared without detergents in blue green algal PSII(−) mutants (Woolf et al., 1994; Di Magno et al., 1995). In this case, the emission maximum is near 690 nm and is associated with the bulk chls. However, in these cases, it is not stated whether the published emission spectra were instrument (phototube) corrected. On the other hand, Holzwarth et al. (1993) show instrumentally corrected emission spectra for detergent-treated core particles which possess a somewhat more prominent red-shifted band.

An interesting feature of the comparison between calculated and measured fluorescence spectra (Figure 9) is the deviation from equilibration detected around 695 nm. As pointed out under Results, we attribute this to a perturbation of the equilibrium distribution of excited states by RC photochemical trapping. Such a perturbation is expected in the case of fast photochemical trapping, as recently pointed out by Laible et al. (1994) on the basis of model calculations. This perturbation, which lowers the fluorescence yield of the primary donor, is expected to be transmitted to the nearest neighbour chlorophylls. Such a situation has been demonstrated to occur in PSII where chlorophylls, which are slightly red shifted with respect to P680, are most strongly coupled energetically to it (Jennings et al., 1991, 1992). In the case of PSI−LHCI, by calculating the absorption band associated with the measured emission spectrum of Figure 9 and comparing it with the measured absorption band, it is possible to estimate that the absorption area intensity, associated with the 695 nm feature, involves a minimum number of 5−6 chls, if one assumes a very low fluorescence yield for these chls. As P700, assumed here to carry a dimer oscillator strength, is expected to be included in this structure, we suggest that at least 3−4 antenna chls, which are slightly blue shifted with respect to P700, are closely associated and strongly coupled to it. This interpretation does not completely exclude the presence of a small number of other chls weakly coupled to P700, e.g., one or two molecules of long-wavelength forms, which transfer directly to P700 at a rate equal to or slower than the overall equilibration time. In this case, the equilibrium fluorescence yield of these red forms would be scarcely affected by proximity to P700, and we would be unable to detect it in this experiment. However, steric factors may severely limit the close presence of such red forms to P700 as we suggest that at least 3−4 blue-absorbing antenna molecules seem to be closely associated with it.

Inspection of the temperature sequence of emission spectra clearly points to the presence of at least three distinct red emission forms near 722, 730, and 740 nm. This latter emission has not previously been detected in higher plant

PSI as far as we are aware, though an even longer wavelength fluorescence band has been detected in *Spirulina platensis* at cryogenic temperatures (Shubin et al., 1995). The three red emission structures are well described over the temperature range employed here, by 15−17 nm wide Gaussians with maxima at 720, 730, and 742 nm. The bandwidths apparently display almost no temperature sensitivity, thus suggesting that each is substantially inhomogeneously broadened. In the case of non-red-shifted antenna spectral forms for PSII chl−protein complexes, the room temperature bandwidths are around 10 nm and are dominated by the homogeneous line width [$(7.7S\nu_m T)^{1/2} \cong 200$ cm^{-1} (Hayes et al., 1988), where S is the electron−phonon coupling, ν_m is the average phonon frequency, and T is the absolute temperature] with an approximately 100 cm^{-1} inhomogeneous broadening (Hayes et al., 1988; Jennings et al., 1994a; Zucchelli et al., 1995b). This generates a readily detectable sensitivity of bandwidth to temperature (Zucchelli et al., 1995b; Cattaneo et al., 1995). Thus, in the case of the red forms, the apparently broad bandwidth (15−17 nm) together with a nondetectable temperature sensitivity suggests, as mentioned above, that the absorption is dominated by a very large inhomogeneous broadening and that the electron−phonon coupling is extremely weak. This conclusion is not in agreement with the recent suggestion that red forms may display very strong electron−phonon coupling (Peterman et al., 1994). However, this latter suggestion was based on the conclusion that the fluorescence Stokes shifts for red forms are very great (10−20 nm). In the present paper, we demonstrate, on the basis of thermodynamic calculations for this thermally equilibrated system, that for the inhomogeneously broadened red bands Stokes shifts are around 4−6 nm. For the purely homogeneously broadened bands, the Stokes shifts (ΔS) will be even smaller, and it is this parameter which yields the coupling strength ($\Delta S \sim 2S\nu_m$), which we therefore expect to be small with an optical reorganization energy ($S\nu_m$) probably not in excess of 10−15 cm^{-1} based on our previous thermal broadening studies of PSII absorption bands (Zucchelli et al., 1995b; Cattaneo et al., 1995).

As mentioned in the introduction, P700 is generally considered to be a "deep trap" in the sense that it is energetically much lower than the bulk antenna. The present observation of a thermally equilibrated fluorescence at RT, in which about 90% of the excited states are associated with the long-wavelength antenna forms, casts some doubt on this traditional point of view. In order to examine this, we have estimated an approximate probability of an exciton being on P700. This was achieved by calculating a homogeneously broadened line width for P700 at RT by using the hole-burning literature values for electron−phonon coupling ($S = 5$) to low-frequency bath phonons ($\nu_m = 20$ cm^{-1}) (Hayes et al., 1988). In this way, the FWHM (FWHM$^2 = 7.7S\nu_m T$) was estimated to be 480 cm^{-1} (24 nm) at RT. We furthermore assumed a Gaussian band shape and the oscillator strength of a chl dimer with an absorption maximum at 700 nm, as is generally accepted. This calculated P700 band is clearly not intended to represent the absorption spectrum of P700 in any detail, but is intended to serve as a useful approximation for the equilibrium calculations. This P700 band was subtracted from the measured absorption spectrum of PSI−LHCI. The calculated equilibrium emission spectra were then estimated for both the measured absorption band and the measured band minus the attributed P700 absorption. These spectra are shown in Figure 10. The hatched area, normalized to the total area, thus approximates the expected equilibrium population of excited states in P700 (obviously in the absence of charge separation) and yields a value of 0.013. The P700 dimer has an absorption weighting of about 0.01 in PSI−LHCI. Thus, the excited state to absorption ratio (S^*/A) is about 1.3. From the expression $\Delta G° = kT \ln (S^*/A)_{P700}/(S^*/A)_{antenna}$, the average free energy for excited state transfer from the antenna to P700 is −0.26 kT at RT. We wish to emphasize that these rather surprisingly low estimated S^*/A and $-\Delta G°$ values are only further decreased in the case of assuming (a) less than the total oscillator strength of chl dimer in the low-energy band at 700 nm or (b) a lower electron−phonon coupling strength ($S < 5$). Thus, it is clear from these considerations that P700 is only slightly lower energetically than its antenna when the red forms are taken fully into account. Previous misconceptions concerning this important point were based on an incomplete appreciation of the role of the red forms.

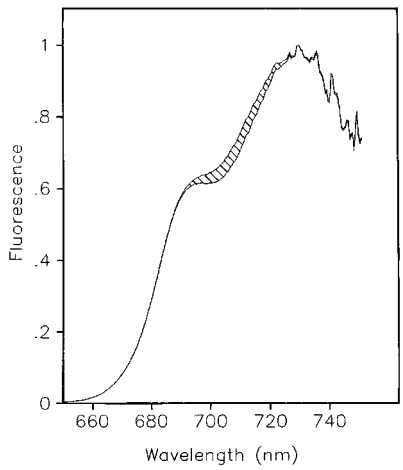

FIGURE 10: Effect of the calculated P700 absorption on the fluorescence emission spectrum estimated by the Stepanov analysis of PSI−LHCI absorption. The upper curve represents the emission spectrum calculated from the measured absorption spectrum. The lower curve represents the calculated emission spectrum after the estimated P700 absorption band had been subtracted from the measured absorption spectrum. The hatched area represents the emission associated with P700. For further details, see text.

It is interesting to note in this context that the equilibrium population of excited states associated with P680 is in the range 0.01−0.02 (Jennings et al., 1994a). Thus, it would seem that despite the marked differences in antenna properties of PSI and PSII, the time-averaged excitation probability of the primary donor is approximately equal for the two photosystems.

This conclusion that P700 is almost isoenergetic with its antenna, as is P680, raises the important problem of the considerable differences in the overall photochemical trapping rate of the two photosystems. For PSII, this is in the 200−300 ps range (Holzwarth et al., 1987; Leibl et al., 1989) while for PSI−LHCI most studies suggest 50−100 ps (Holzwarth, 1986; Hodges & Moya, 1986; Owens et al., 1987; Turconi et al., 1994). This point has been previously discussed (Trissl, 1993; Jennings et al., 1996). For a thermalized situation, the primary trapping rate (k_{tr}) is given by $k_{tr} = [P^*]k_{cs}$ where $[P^*]$ is the equilibrium population of excited states on the primary donor and k_{cs} is the primary charge separation rate constant. If we take an "average" value for $k_{tr} = (80 \text{ ps})^{-1}$ from the literature (in agreement with the fluorescence yield of 0.5% determined for this PSI−

LHCI particle; see Materials and Methods) and [P*] = 0.013, we calculate $k_{cs} = 1$ ps^{-1}. We believe this to be a lower limit for k_{cs} as it is based on the assumption that all the oscillator strength of the P700 is in the lower energy exciton state at 700 nm. Thus, a more reasonable suggestion would put k_{cs} in the 1−2 ps^{-1} range. For PSII, the k_{cs} of P680 is generally considered to be around 0.3−0.5 ps^{-1} (Schatz et al., 1988). We therefore suggest that the main reason for the fast PSI trapping rate is to be found in its extremely fast primary charge separation rate. Extremely fast primary charge separation in PSI has previously been suggested by Trinkunas and Holzwarth (1994) on the basis of kinetic modeling. We point out that if the k_{cs} value is really in the subpicosecond range, it is probably not unreasonable to think that trapping will occur with a high probability upon P700 excitation. This means that little back-transfer to the antenna may occur and the overall trapping time of about 100 ps may well be similar to the first antenna−P700 passage time and hence to a substantially diffusion-limited situation.

ACKNOWLEDGMENT

We thank Dr. Birger Lindberg Møller and Dr. Stefan Jansson for their generous gift of antibodies.

REFERENCES

Arnon, D. I. (1949) *Plant Physiol. 24*, 1−15.
Baron, C., & Thompson, T. E. (1975) *Biochim. Biophys. Acta* 382−385.
Bassi, R., & Simpson, D. (1987) *Eur. J. Biochem. 163*, 221−230.
Bassi, R., Machold, O., & Simpson, D. (1985) *Carlsberg Res. Commun. 50*, 145−162.
Bassi, R., Hoyer-Hansen, G., Barbato, R., Giacometti, G. M., & Simpson, D. J. (1987*) J. Biol. Chem. 262*, 13333−13341.
Bassi, R., Giacometti, G. M., & Simpson, D. J. (1988) *Biochim. Biophys. Acta 935*, 152−165.
Boekema, E. J., Wynn, R. M., & Malkin, R. (1990) *Biochim. Biophys. Acta 1017*, 49−56.
Bruce, B. D., & Malkin, R. (1988) *J. Biol. Chem. 263*, 7302−7308.
Cattaneo, R., Zucchelli, G., Garlaschi, F. M., Finzi, L., & Jennings, R. C. (1995) *Biochemistry* 34, 15267−15275.
Chitnis, P. R., Xu, Q., Chitnis, V. P., & Neushtai, R. (1995*) Photosynth. Res*. 44, 23−40.
Di Magno, L., Chan, C.-K., Jia, Y., Lang, M. J., Newman, J. R., Mets, L., Fleming, G. R., & Helselkorn, R. (1995) *Proc. Natl. Acad. Sci. U.S.A. 92*, 2715−2719.
Gobets, B., van Amerongen, H., Monshouwer, R., Kruip, J., Rögner, M., van Grondelle, R., & Dekker, J. P. (1994) *Biochim. Biophys. Acta 1188*, 75−85.
Golbeck, J. H. (1992) *Annu. Rev. Plant Physiol. Plant Mol. Biol. 43*, 293−324.
Hastings, G., Kleinherenbrink, F. A. M., Lin, S., & Blankenship, R. E. (1994) *Biochemistry* 33, 3185−3192.
Hayes, J. M., Gillie, J. K., Tang, D., & Small, G. J. (1988) *Biochim. Biophys. Acta 932*, 287−305.
Hodges, M., & Moya, I. (1986) *Biochim. Biophys. Acta* 849, 193−202.
Holzwarth, A. R. (1986) *Photochem. Photobiol. 43*, 707−725.
Holzwarth, A. R., Brock, H., & Schatz, G. H. (1987) *Prog. Photosynth. Res. 1*, 67−69.
Holzwarth, A. R., Schatz, G., Brock, H., & Bittersmann, E. (1993) *Biophys. J. 64*, 1813−1826.
Ide, J. P., Klug, D. R., Kühlbrandt, W., Giorgi, L. B., & Porter, G. (1987) *Biochim. Biophys. Acta 893*, 349−364.
Jennings, R. C., Zucchelli, G., & Garlaschi, F. M. (1991) *Biochim. Biophys. Acta* 1060, 245-250.
Jennings, R. C., Zucchelli, G., Garlaschi, F. M., and Vianelli, A. (1992) *Biochim. Biophys. Acta* 1101, 79−83.
Jennings, R. C., Bassi, R., Garlaschi, F. M., Dainese, P., & Zucchelli, G. (1993) *Biochemistry* 32, 3203−3210.
Jennings, R. C., Garlaschi, F. M., Finzi, L., & Zucchelli, G. (1994a) *Lith. J. Phys. 34*, 293−300.
Jennings, R. C., Zucchelli, G., Bassi, R., Vianelli, A., & Garlaschi, F. M. (1994b) *Biochim. Biophys. Acta 1184*, 279−283.
Jennings, R. C., Garlaschi, F. M., Finzi, L., & Zucchelli, G. (1996) *Photosynth. Res. 47*, 167−173.
Laible, P. D., Zipfel, W. & Owens, T. G. (1994) *Biophys. J. 66*, 844−860.
Lam, E., Ortiz, W., & Malkin, R. (1984) *FEBS Lett. 168*, 10−14.
Leibl, W., Breton, J., Deprez, J., & Trissl, H.-W. (1989) *Photosynth. Res*. 22, 257−275.
Mukerji, I., & Sauer, K. (1989) *Curr. Res. Photosynth. 2*, 321−324.
Mukerji, I., & Sauer, K. (1993) *Biochim. Biophys. Acta 1142*, 311−320.
Mullet, J. E., Burke, J. J., & Arnon, C. J. (1980) *Plant Physiol. 65*, 823−827.
Nechushtai, R., Nourizadeh, S. D., & Thornber, J. P. (1986) *Biochim. Biophys. Acta* 848, 193-200.
Owens, T. G., Webb, S. P., Mets, L. J., Alberte, R. S., & Fleming, G. R. (1987) *Proc. Natl. Acad. Sci. U.S.A.* 84, 1532−1536.
Pålsson, L. O., Tjus, S. E., Andersson, B., & Gillbro, T. (1995) *Chem. Phys. 194*, 291−302.
Petermam, E. J. G., Dekker, J. P., van Grondelle, R., van Amerongen, H., & Nussberger, S. (1994) *Lith. J. Phys. 34*, 301−305.
Porra, R. J., Thompson, W. A., & Kriedermann, P. E. (1989) *Biochim. Biophys. Acta 975*, 384−394.
Ross & Calvin (1967) *Biophys. J. 7*, 595−614.
Ruban, A. V., & Horton, P. (1992) *Biochim. Biophys. Acta* 1102, 30−38.
Schägger, H., & von Jagow, G. (1987) *Anal. Biochem*. 166, 368−379.
Schatz, G. H., Brock, H, & Holzwarth, A. R. (1988) *Biophys. J*. 54, 397−405.
Seely, G. R., & Connolly, J. S. (1986) in *Light Emission by Plants and Bacteria* (Govindjee, Amesz, J., & Fork, D. C., Eds.) pp 99−133, Academic Press, Inc., Orlando, FL.
Shubin, V. V., Bezsmertnaya, I. N., & Karapetyan, N. V. (1995) *J. Photochem. Photobiol*. 99, 1−8.
Sieferman-Harms, D., & Ninneman, H. (1982) *Photochem. Photobiol*. 35, 719−731.
Sopko, B., Sofrovà, D., Hladik, J., Gulyayev, B. A., & Tetenkin, V. L. (1995) in *Photosynthesis: from Light to Biosphere* (Mathis, P., Ed.) Vol. 2, pp 47−50, Kluwer Academic Publishers, Dordrecht.
Stepanov, B. I. (1957) *Sov. Phys. Dokl*. 2, 81−84.
Tjus, S. E., & Andersson, B. (1991*) Photosynth. Res*. 27, 209−219.
Trinkunas, G., & Holzwarth, A. R. (1994*) Biophys. J*. 66, 415−429.
Trissl, H.-W. (1993*) Photosynth. Res*. 35, 247−263.
Turconi, S., Weber, N., Schweitzer, G., Strotmann, H., & Holzwarth, A. R. (1994*) Biochim. Biophys Acta* 1187, 324−334.
Werst, M., Jia, Y., Mets, L., & Fleming, G. R. (1992) *Biophys. J. 61*, 868−878.
Wittmershaus, B. P. (1986) *Progress in Plant Research* (Biggins, J., Ed.) Vol. 1, pp 75−82, Martinus Nijhoff Publishers, Dordrecht.
Woolf, V. M., Wittmershaus, B. P., Vermaas, W. F. J., & Tran, T. D. (1994) *Photosynth. Res.* 40, 21−34.
Zscheile, F. P., & Harris, D. G. (1947) *J. Phys. Chem. 47*, 623−630.
Zucchelli, G., Jennings, R. C., & Garlaschi, F. M. (1990*) J. Photochem. Photobiol. B: Biol. 6*, 381−394.
Zucchelli, G., Jennings, R. C., & Garlaschi, F. M. (1992) *Biochim. Biophys. Acta 1099*, 163−169.
Zucchelli, G., Garlaschi, F. M., Croce, R., Bassi, R., & Jennings, R. C. (1995a) *Biochim. Biophys. Acta 1229*, 59−63.
Zucchelli, G., Garlaschi, F. M., Finzi, L., & Jennings, R. C. (1995b) in *Photosynthesis: from Light to Biosphere* (Mathis, P., Ed.) Vol. 1, pp 179−182, Kluwer Academic Publishers, Dordrecht.

BI960214M